〈Invited Paper〉
Journal of Korean Institute of surface Engineering
Vol. 29, No. 5, Oct., 1996

PREFERRED ORIENTATION OF TIN FILM STUDIED BT A REAL TIME SYNCHROTRON X-RAY SCATTERING

J. H. Je* and D. Y. Noh**

**Dept. of Matls Sci. & Eng., Pohang University of Science & Technology, Korea*
***Dept. of Matls Sci. & Eng., Kwangju Institute of Science & Technology, Korea*

ABSTRACT

The orientational cross-over phenomena in an RF sputtering growth of TiN films were studied in an *in-situ*, real-time synchrotron x-ray scattering experiment. For the films grown with pure Ar sputtering gas, the cross-over from the more strained (002)-oriented grains to the less strained (111)-oriented grains occurred as the film thickness was increased. As the sputtering power was increased, the cross-over thickness, at which the growth orientation changes from the <002> to the <111> direction, was decreased. The addition of N_2 besides Ar as sputtering gas suppressed the cross-over, and consequently resulted in the (002) preferred orientation without exhibiting the cross-over. We attribute the observed cross-over phenomena to the competition between the surface and the strain energy. The x-ray powder diffraction, the x-ray reflectivity, and the *ex-situ* AFM surface topology study consistently suggest that the microscopic growth front was in fact always the (002) planes. In the initial stage of growth, the (002) planes were aligned to the substrate surface to minimize the surface energy. At later stages, however, the (002) growth front tilted away from the surface by about 60° to relax the strain, which caused the cross-over of the preferred growth direction to the <111> direction.

INTRODUCTION

Understanding morphology of thin film growth fronts is quite a challenge both experimentally and theoretically. In this study, we are particularly interested in the change of the preferred growth orientation, the crystalline axis direction along the global growth direction, during growth process. Cross-over phenomena of the preferred growth orientation have been observed in systems such as TiN[1-3] and Ag[4]. Although the cross-over phenomena are believed to be a result of kinetic constraints in the growth conditions that are far from thermodynamic equilibrium, the microscopic mechanism is not well understood.

TiN films grown by vapor phase deposition techniques usually have a preferred growth orientation that varies according to growth conditions[1, 5-7]. Most explanations suggested on the preferred orientation in thin films were given in terms of the surface energy of the film and kinetic factors[1, 8-11]. It was pro

(Electronic mail : jhje@vision.postech.ac.kr)

posed in the case of TiN films that the atoms arrange themselves into the plane of the lowest surface energy, e.g., the (111) plane in equilibrium conditions, while they might form a plane of higher energy, e. g., the (002) plane in non-equilibrium conditions[1, 6)]. However, such explanations have a few problems. The first is that the plane of the lowest surface energy is not the (111), but the (002) plane in TiN crystal with the NaCl-type structure[12)]. The second problem is that the change in the preferred orientation with the film thickness cannot be described with only the surface energy and kinetics[2]. Therefore, another driving force that causes the preferred orientation of TiN films should be investigated.

Recently, Oh and Je[2], using their cross-sectional TEM results, observed the critical thickness suggested by Pelleg et al.[12)], below which the film had the <002> preferred orientation and above which the <111> preferred orientation. However, the detailed nature of the transformation of the growth direction remains elusive due to the limitations of the *ex-situ* x-ray and TEM studies involved.

In this work, we report a series of real time synchrotron x-ray measurement to reveal the nature of the growth morphology of TiN films grown by RF sputtering. In a real time x-ray scattering experiment, successive measurements of x-ray scattering profiles are performed, while the growth is in progress.

EXPERIMENTAL DETAILS

The TiN films were grown onto Si(001) substrates by radio frequency (RF) magnetron sputtering in an x-ray sputtering chamber in which a TiN target (1 inch diameter) was placed 10 cm away from the substrate as shown in Fig. 1(a). The sputtering chamber was equipped with a Be window that is mostly transparent to x-rays. In this work, the sputter gun was operated with RF power between 6 W/㎠ to 12 W/㎠. As carrier gases, we used either 5×10^{-3} Torr Ar (99.9999%), or a mixture of 5×10^{-3} Torr Ar and 1.5×10^{-3} Torr N_2(99.9999%). The base pressure of the chamber was below 2×10^{-6} Torr and the substrate temperature was fixed at 100 C.

The X-ray experiment was carried out at

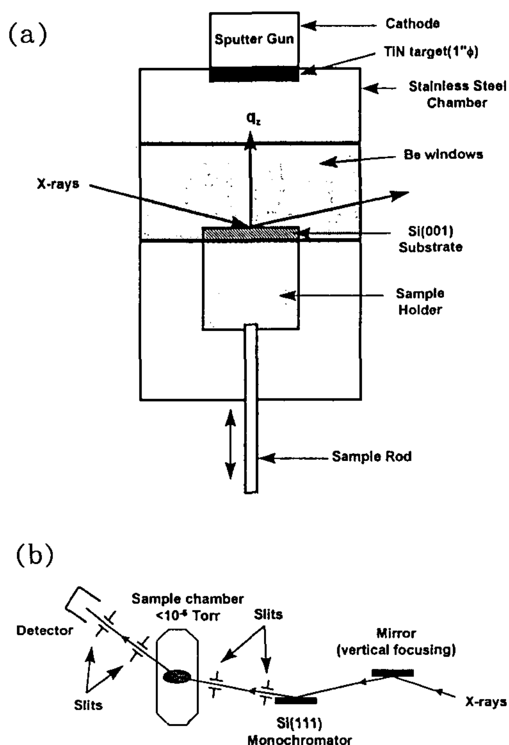

Fig. 1 Schematic diagram of (a) an x-ray sputtering chamber for *in-situ*, real-time synch-rotron x-ray scattering experiments, and (b) x-ray scattering setup at X10B, NSLS.

Exxon beamline X10B at the National Synchrotron Light Source. The incident X-rays from the bending magnet were focused horizontally, and monochromatized to 11 keV by a bent Si(111) crystal. The X-ray scattering setup is shown in Fig. 1(b) schematically. Typical momentum transfer resolution of the experiment was set at $0.001\,Å^{-1}$. To achieve the exact scattering geometry, we placed the sputtering chamber on a four-circle x-ray diffractometer that enables us to attain arbitrary momentum transfer q in three-dimensional space. The detailed scatt-ering geometry using a four-circle diffractometer has been well described in Ref. 13.

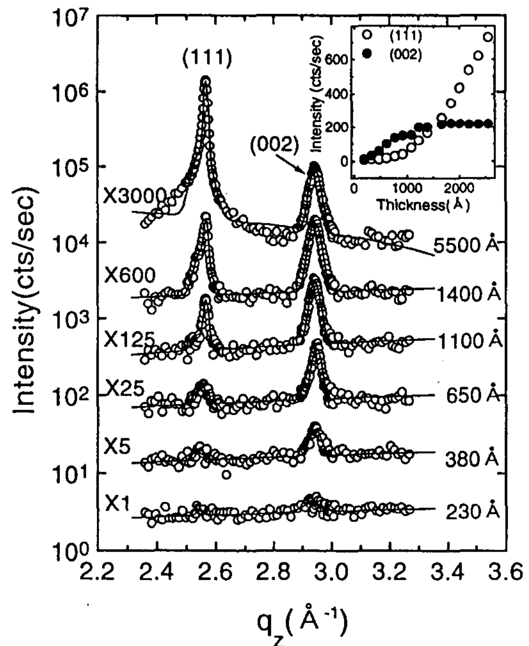

Fig. 2 A series of diffraction patterns along the surface normal q_z direction taken in real time on the sample grown at 10W/㎠. The data were multiplied by appropriate factors for clear illustration. The solid lines are results of fit to a sum of Gaussians. The inset shows the peak intensities of both the (111) and the (002) reflections versus the film thickness. Note that the data are plotted in a logarithmic scale.

CROSS-OVER OF THE PREFERRED GROWTH DIRECTION

Orientational cross-over with increasing film thickness

We first discuss the data obtained on a film grown under the RF power of 10W/㎠ with pure 5×10^{-3} Torr Ar carrier gas in detail. The growth rate, that was estimated from the real time x-ray reflectivity, was~6 Å/min. The film thickness at a specific instant is given by $2\pi/\Delta q$ 14, where Δq is the period of the intensity oscillations in the reflectivity curves.

A typical set of powder x-ray diffraction profiles obtained during the growth is shown in Fig. 2. It includes a series of scans along the substrate surface normal, q_z direction obtained at different times (expressed in film thickness). The scattering intensity was expressed in a logarithmic scale for better comparison between the (111) Bragg reflection and the (002) Bragg reflection. Noting that bulk TiN has a cubic structure with the (111) Bragg reflection at $2.568\,Å^{-1}$ and the (002) at $2.963\,Å^{-1}$, the figure readily illustrates that the cross-over of the growth orientation from the<002> direction to the <111> direction occurs as the film thickness increases. This result is consistent with the previous reports by ex-situ XRD and TEM studies[2, 3].

To illustrate the cross-over clearly, we plotted the peak intensities of both the (111) and the (002) reflections versus the film thickness in the inset of Fig. 2. This shows the cross-over from the <002> to the <111>

direction vividly. As we examined the details of the diffraction data, we noticed that during the very early stage of the film growth (film thickness < 230 Å), the intensity ratio of Bragg peaks was similar to that of a complete powder film with random crystalline orientation. This indicated that the nucleation and the early stage growth took place in random orientations. Following the early random orientation growth, the deposition was proceeded by the predominant growth of the grains with the (002) crystallographic plane parallel to the substrate surface. This was signified by the rapid increase of the (002) peak intensity until the film thickness reached about 1000 Å. After this stage, the (002) peak intensity became saturated, and the intensity of the (111) peak began to increase rapidly. This indicated that the grains with the <111> crystallographic orientation parallel to the substrate normal became dominant at this stage. The growth direction crossed over from the <002> direction to the <111> direction.

The effect of the sputtering power on the cross-over

We now discuss the X-ray diffraction profiles obtained during the film growth at various RF sputtering powers keeping other growth conditions identical to those described in the previous section. The data obtained at the sputtering powers of 6W/㎠, 10W/㎠, and 12W/㎠, are illustrated in Fig. 3(a), 3(b), and 3(c) respectively. We note that the data set in Fig. 3(b) was the same set as that discussed in the previous section, plotted in a linear scale. Each figure includes a series of scans taken along the surface normal, qz direction at different thicknesses. As is obvious from the Fig. 3, all the films show the cross-over of the growth orientation from the <002> to the <111> directions with increasing film thickness. In addition, the data in Fig. 3 showed that the cross-over thickness was decreased as the RF sputtering power was raised. At the highest RF power of 12W/㎠ the (111) growth became dominant from the very beginning of the deposition as shown in Fig. 3(c).

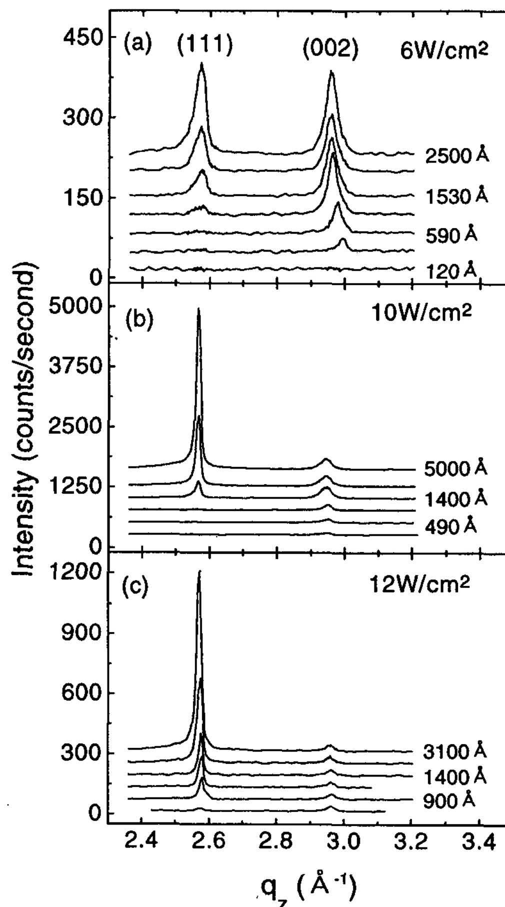

FIG. 3. The powder X-ray scattering patterns obtained during the film growth at various RF sputtering powers of, (a) 6W/㎠, (b) 10 W/㎠, and (c) 12 W/㎠.

The effect of the N_2 carrier gas on the cross-over

Fig. 4(a) and 4(b) show the x-ray diffraction profiles obtained during the film growth for the TiN films that were sputtered at 12W/㎠ with mixture of 5×10^{-3} Torr Ar and 1.5×10^{-3} Torr N_2 (a), and with 5×10^{-3} Torr Ar (b). We note that the data set on Fig. 4(b) are the same one as shown in Fig. 3(c). The figure illustrated the effect of the additional N_2 carrier gas clearly. The cross-over to the <111> preferred orientation did not occur on the film grown with the addition of the N_2 gas at all, and the (002)-oriented grains were dominant even at later stages. The <002> preferred growth direction induced by increasing the nitrogen partial pressure has been reported in TiN films previously[15,16]. The evolution of the peak intensities in each case was shown in Fig. 4(c) and 4(d).

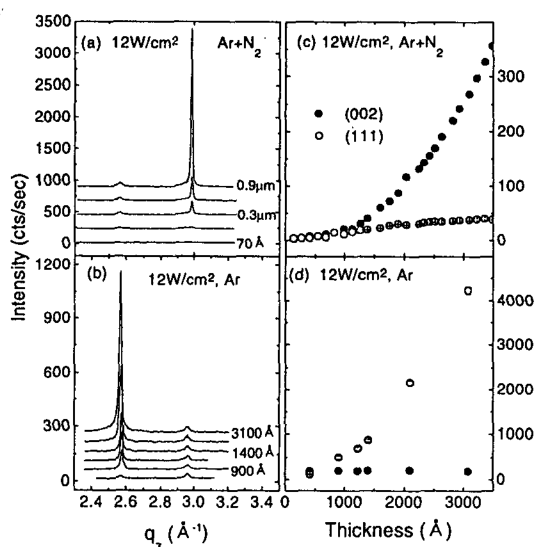

FIG. 4. (a) The X-ray diffraction profiles obtained during the growth for the films that were sputtered at 12W/㎠ with the mixture of 5×10^{-3} Torr Ar and 1.5×10^{-3} Torr N_2. The (002) peak was dominant at all thicknesses. (b) The X-ray diffraction profiles obtained during the growth for the films that were sputtered at 12W/㎠ with 5×10^{-3} Torr Ar. The (111) peak was dominant from the beginning of the growth. (c, d) The intensities of the Bragg reflections shown in (a) and (b).

THE DETAILED PROCESS OF THE ORIENTATIONAL CROSS-OVER

The film growth was likely to be carried out by completing crystal planes with low surface energy such as the (002) or the (111) planes as the growth front. Based on this, two scenarios (schematically illustrated in Fig. 5(a)) are possible for the growth front of the grains that causes the (111) reflection in the late stage of growth. The first

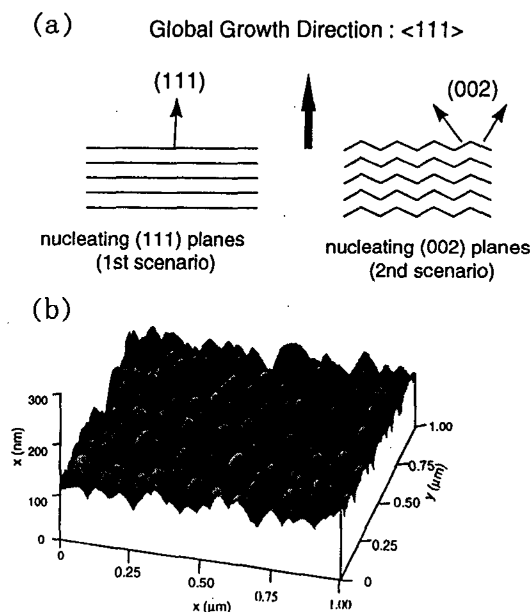

FIG. 5. (a) A schematic illustration of the possible configurations of the late stage growth discussed in the text. (b) An AFM image of the final surface topology. The surface was faceted into facets tilted by 50° ± 15° away from the surface normal.

is the nucleation of the (111) crystal planes parallel to the surface. In this case, the growth front crosses over from the energetically favorable (002) planes to the (111) planes as proposed in the previous *ex-situ* x-ray diffraction studies[2]. The second possibility is that the film still grows by locally completing the (002) planes that are tilted away from the surface by about 60° Even in this case, the global growth direction is still along the substrate normal close to the <111> direction. Although the (111) reflection occurs close to the surface normal in both cases, the growth mechanism and the resulted surface morphology are quite different.

To address the above issue, we studied the final surface topology after the growth in an *ex-situ* Atomic Force Microscopy (AFM) measurement. The AFM picture shown in Fig. 5(b) illustrates that the final state surface was consisted of a hill-and-valley structure of facets that are inclined about 50° ± 15° to the surface normal. This is qualitatively consistent with the second scenario where the local growth front is the (002) planes tilted by 60° off the surface normal.

To be more quantitative on the final state surface topology, we measured the rocking curve for the specular (111) reflection in Fig. 2 as demonstrated in Fig. 6(a). It shows the mosaic distribution of the (111) planes near the out-of-plane direction. To obtain the detailed information of the preferred growth orientations, one needs to observe additional Bragg reflections lying on the off-specular directions, the directions other than the specular direction, as well as the corresponding rocking curves of the Bragg reflection. We could find out the off-specular (002) reflec

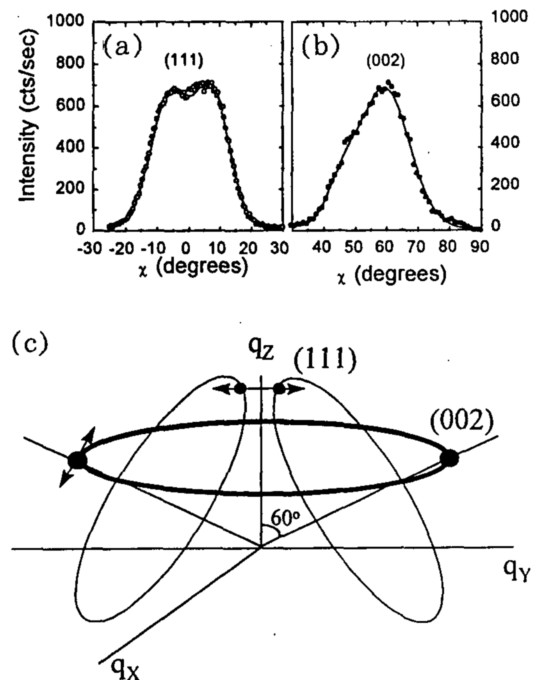

FIG. 6. (a) The diffraction profile taken by rocking the sample at the specualr (111) reflection. The profile was described by a double Gaussian peak at ±5° away from the surface normal. (b) The rocking curve of the off-specular (002) reflection. (c) The schematic diffraction profile of the second scenario described in the text in the reciprocal space.

tion at the position where the momentum transfer is 54.7° off from the surface normal. (The off-specular (002) reflection should not be confused with the specular (002) reflection in Fig. 2.) Fig. 6(b) shows the rocking curve of the off-specular (002) reflection where the sample was rocked while the magnitude of the momentum transfer is held at the position of the off-specular (002) reflection. It is interesting that the maximum peak of the (002) reflection was found at 60° off rather than at 54.7° from the surface normal. Since the angle between the <111> and the

<002> direction is 54.7°, we conclude that the specular (111) and the off-specular (002) reflections in Fig. 6(a) and 6(b) are originated from identical grains (grown at later stages). There are two important features that may cast clues to resolve the growth morphology. The first is that the rocking curve of the specular (111) reflection consisted of two Gaussian curves peaked at±5° off from the surface normal (Fig. 6 (a)), which also explains the maximum peak of the off-specular (002) reflection at 60° in Fig. 6(b). The second is that the two rocking curves have similar peak intensity. In case of nucleating the (111) plane parallel to the surface (the first scenario), one would expect to see a single Gaussian distribution of the (111) direction near the surface normal. Also the peak intensity of the off-specular (002) reflection would be much smaller than that of the (111) reflection, since the (002) reflection would be isotropically distributed on the azimuthal circle while the (111) reflection is concentrated in the surface normal direction. We note that the TiN grains did not have any azimuthal epitaxial relation to the substrate. On the other hand, in the second scenario, the grains are grown along the <002> direction that is tilted away from the surface normal by 60°. Again in the plane, the off-specular (002) reflection would be distributed isotropically on the azimuthal circle shown in Fig. 6 (c) by a thick solid line. The associated (111) reflection from each grain, the (111) reflection from the grain generating the (002) reflection in the off-specular direction, would then be distributed on the circles represented by thin solid line. Although it requires a quantitative comparison of the integrated intensities to be exact, it is plausible that the (111) peak and the (002) peak have similar intensity in this case. On this basis, we believe that the late stage growth was proceeded by the growth of the grain with the (002) growth front tilted by 60° away from the surface normal.

CONCLUDING REMARKS

In this work, we report a real-time synchrotron x-ray measurement that revealed the details of the orientational cross-over in TiN films grown by RF sputtering. Following the initial random nucleation and growth stage, the growth was first dominated by the grains with the (002) planes aligned with the substrate surface. In the later stage, the growth was proceed by the growth of the grains with the (002) front tilted away from the surface by about 60°. We explain the observed cross-over with the lattice strain induced in the film growth process.

ACKNOWLEDGEMENT

This work was supported by Korean Ministry of Education through Research Fund for Advanced Materials in 1995 (J. H. Je), KOSEF-961-0209-105-2 (D. Y. Noh).

REFERENCES

1. D. S. Rickerby, A. M. Jones, and B. A. Bellamy, Surf. Coat. Technol. **37**, 4375 (1989).
2. U. C. Oh and J. H. Je, J. Appl. Phys. **74**, 1692 (1993).
3. U. C. Oh, J. H. Je and J. Y. Lee, J. Mater.

Res. 10, 634 (1995).

4. P. K. Dutta and H. William, J. Phys. D : Appl. Phys. 3, 839 (1970).
5. M. Kobayashi and Y. Doi, Thin Solid Films 111, 259 (1984).
6. J. -E. Sundgren, Thin Solid Films 128, 21 (1985).
7. J. I. Jeong, J. H. Hong, J. S. Kang, H. J. Shin, and Y. P. Lee, J. Vac. Sci. Technol. A9, 2618 (1991).
8. S. Veprek, Thin Solid Films 130, 135 (1985).
9. D. Walton, T. N. Rhodin and R. W. Rollins, J. Chem. Phys. 38, 2698 (1963).
10. D. N. Lee, J. Mater. Sci. 24, 4375 (1989).
11. A. Gittis and D. Dobrev, Thin Solid Films 130, 335 (1985).
12. J. Pelleg, L. Z. Zevin, and S. Lungo, Thin Solid Films 197, 117 (1991).
13. W. R. Busing and H. A. Levy, Acta. Cryst. 22, 457 (1967).
14. D. Y. Noh, Y. Hwu, H. K. Kim, and M. Hong, Phys. Rev. B 51, 4441 (1995).
15. J. -E. Sundgren, B.-O. Johansson, S.-E. Karlsson and H. T. G. Hentzell, Thin Solid Films 105, 367 (1983).
16. V. Valvoda, R. Kuzel, Jr. And R. Cerny, Thin Solid Films 156, 53 (1988).